

EFFECT OF AROMATIC OIL ON PHASE DYNAMICS OF S-SBR/BR BLENDS FOR PASSENGER CAR TIRE TREADS

A. Rathi*^a, M. Hernández^b, W.K. Dierkes^a, J.W.M. Noordermeer^a, C. Bergmann^c,
J. Trimbach^c and A. Blume^a

^aUniversity of Twente, Dept. of Elastomer Technology and Engineering, P.O. Box 217, 7500
AE Enschede, The Netherlands

^bDelft University of Technology, Faculty of Aerospace Engineering, Novel Aerospace Materials
Group, Kluyverweg 1, 2629 HS Delft, The Netherlands

^cHansen & Rosenthal KG, Am Sandtorkai 64, 20457 Hamburg, Germany

Presented at the Fall 190th Technical Meeting of the Rubber
Division of the American Chemical Society, Inc.
Pittsburgh, PA
October 12, 2016

ISSN: 1547-1977

* Speaker

ABSTRACT

S-SBR (solution styrene-butadiene copolymer rubber) / BR (polybutadiene rubber) blends are used in applications like tires, but little is known about the phase dynamics arising from local morphological variations. Information on dynamics of different phases in blends as well as understanding the effect of additives like process oils on polymer dynamics are crucial. The present study aims the understanding of influence mineral-based aromatic process oil's influence (0-20 phr) on the dynamics of the individual phases in a S-SBR/BR (50/50) blend, and its partitioning towards either phase. Differential Scanning Calorimetry, Dynamic Mechanical Analysis, and Broadband Dielectric Spectroscopy are employed to study the α -relaxation (glass transition temperature, T_g) process of the individual phases in the blends. It is shown that the effect of the oil is more significant on the BR phase than on the S-SBR phase, restricting the phase dynamics. A theoretical perspective is added based on the Lodge and McLeish model.

Key words: S-SBR/BR blends, aromatic oil, phase dynamics, glass transition temperature.

1. INTRODUCTION

For a tire, high performance requirements need to be met by the tread. The tread is the outer layer of the tire which makes the only direct contact of the car with the surface of the road. To optimize the overall performance of a tire tread, it is common to vary the type of elastomer(s), amount(s) and type(s) of filler(s), processing aids and vulcanization system. An adequate tire performance can commonly be achieved by using blends of two or three different types of elastomers for a tire tread.

Elastomer blends can be classified into two main categories: Miscible and Immiscible blends. Both have found useful applications in tire treads. For example, miscible SBR (styrene-butadiene copolymer) / BR (polybutadiene) blends [1-3] are used in state-of-the-art tire treads due to the advantageous set of traction, wear and rolling resistance; immiscible IR (polyisoprene) / NR (natural rubber) blends [4] are used due to the improved wet-skid resistance. These examples illustrate that miscible and immiscible blends exhibit dissimilar advantages for tire performance. Depending on blend miscibility behavior, there are changes in tire performance.

There are two main constraints for making a miscible SBR/BR blend design with predictable properties: (i) Lack of knowledge about the partitioning of processing aids and other compounding ingredients in the individual phases of these blends; it is expected that the processing aids may prefer either of these elastomers based on the 'like dissolves like' principle, since there is a considerable difference in the polarities of SBR and BR; (ii) Thermorheological complexity which arises due to the T_g of SBR and BR being very different from each other. A thermorheologically simple polymer system is one in which the molecular mechanisms contributing to time and frequency dependent modulus and compliance functions, have the same temperature

dependence [5]. Due to the thermorheological complexity of blends the Time-Temperature Superposition (TTS) concept cannot be applied. Therefore, it is necessary to apply more sophisticated techniques to study blend dynamics. Techniques like broadband dielectric spectroscopy [6-13], neutron spin-echo [14,15], and NMR spectroscopy [16-22] can be suitable for this purpose.

The mineral-based aromatic process oil: Treated Distillate Aromatic Extract (TDAE), is known to attribute various advantageous properties such as energy saving, improving homogeneity, increase filler loading and a plasticising effect on the elastomer compounds. The shift in the glass transition temperature T_g is commonly taken to evaluate the plasticising efficiency of the process oil [23]. Therefore, the goal of the present research is to study the T_g by means of Differential Scanning Calorimetry (DSC), Dynamic Mechanical Analysis (DMA) and Broadband Dielectric Spectroscopy (BDS). The focus is to develop an understanding of the phase dynamics of the individual S-SBR and BR phase in a S-SBR/BR 50/50 ratio blend for different concentrations of TDAE. DSC, DMA and BDS have different governing principles, which provide an opportunity to study phase dynamics of the blends through different approaches. DSC estimates T_g based on the calorimetric principle, utilizing the pseudo-second order nature of the T_g process. DMA is a dynamic-mechanical approach, which involves the measurement of material specific moduli, loss (E'') modulus and storage (E') modulus, the ratio(E''/E') of which may be used as an indicator of T_g . The DSC-method is able to estimate the T_g only at a hypothetically low frequency of ca. 10^{-3} Hz. Although a frequency sweep is possible with the DMA-method, the frequency is limited to max. 10^2 Hz [24]. In this respect, BDS is known as a more efficient and sensitive technique compared to both, DSC and DMA. BDS allows the investigation of the

various relaxations of a polymeric system, which take place on extremely different time scales in a broad frequency and temperature range in a single run. The main principle of BDS is the sensitivity to fluctuations of molecular dipoles within the system. These fluctuations are related to the molecular mobility of groups, segments or whole polymer chains, which can be observed as different polymeric relaxation processes [25].

The study of phase dynamics in the blend, arising from the individual S-SBR and BR phases, can provide valuable contributions towards the understanding of partitioning of processing oil in an elastomeric compound. A subsequent quantification of the partitioning of TDAE gives an indication of the phase preferences of compounding ingredients, which are the major determinants of the final rubber properties. The effect of varying concentrations of TDAE on the segmental dynamics of the individual phases, S-SBR and BR in the 50/50 blend is considered to be related to the level of compatibility between the polymers, S-SBR, BR and TDAE oil, respectively. Finally, the experimentally obtained results are compared to calculated ones based on the theory about phase dynamics of miscible blends by Lodge and McLeish [26].

2. EXPERIMENTAL

2.1 Materials

The materials used in this study are S-SBR: SPRINTAN™ SLR 4602 (*Trinseo Deutschland GmbH*, Schkopau, Germany); BR: BUNA CB24 (*Arlanxeo Deutschland GmbH*, Leverkusen, Germany) and Treated Distillate Aromatic Extract (TDAE): VIVATEC 500 (*Hansen & Rosenthal KG*, Hamburg, Germany). Some important analytical properties of the S-SBR, BR and TDAE are presented in Table I. The curing

system employed consists of zinc oxide, stearic acid and sulfur from *Sigma Aldrich* (St. Louis, USA); N-cyclohexyl-2-benzothiazole sulfenamide (CBS) from *Flexys* (Brussels, Belgium). All chemical reagents were used as received.

2.2 Mixing

The basic formulation used for this study is presented in Table II, expressed in parts per hundred parts of rubber (phr). The compounds were prepared following a 2-step mixing procedure, with a first stage in an internal mixer. The vulcanization system was added to the mix in a second stage, carried out on a two-roll mill: Table III. The compounds are referred to as S-SBR/BR (50/50)_{0/10/20}, where 0/10/20 are the respective amounts of TDAE in the compounds. The individual components in the blends are referred to as S-SBR/BLEND_{0/10/20} or BR/BLEND_{0/10/20}.

2.3 Curing

The samples were vulcanized in a hydraulic press *Wickert WLP 1600* at 100 bar and 160 °C as sheets with a thickness of 2 mm, according to their $t_{c,90} + 2$ min optimum vulcanization times. The $t_{c,90}$ was determined with a Rubber Process Analyzer *RPA 2000*, *Alpha Technologies*, following ISO 3147:2008 at 160 °C. 0.1-0.2 mm thick sheets were also vulcanized according to their respective $t_{c,90}$ values at 160 °C for BDS measurements.

2.4 Differential Scanning Calorimetry

A Differential Scanning Calorimeter (DSC) *DSC214 Polyma* from *Netzsch* was used to obtain the 'static' glass transition temperature of the vulcanized samples, using a cooling rate of 10 °C/min, from 20 °C down to -150 °C.

2.5 Dynamic Mechanical Analysis

Dynamic Mechanical Analysis (DMA) of the vulcanized samples was done in tension mode in a *Metravib DMA2000* dynamic spectrometer in order to measure the 'dynamic' glass transition temperature. The measurements were performed from -150 °C to +80 °C in steps of five degrees at a dynamic strain of 0.5% and frequency of 1 Hz.

2.6 Broadband Dielectric Spectroscopy

Broadband Dielectric Spectroscopy (BDS) measurements were performed on a Broadband Dielectric Spectrometer with an *ALPHA-A High Performance Frequency Analyzer* of *Novocontrol Technologies*. The vulcanized 0.1-0.2 mm sheets were cut in a disk shape and were mounted in the dielectric cell between two parallel gold plated electrodes. The complex dielectric permittivity ϵ^* ($\epsilon^* = \epsilon' - i\epsilon''$), being composed of ϵ' as the real part and ϵ'' the imaginary part, was measured by performing consecutive isothermal frequency sweeps (10^{-1} - 10^7 Hz) in the temperature range from -120 °C to +80 °C in steps of 5 °C.

3. RESULTS AND DISCUSSION

3.1 Analysis of the S-SBR/BR (50/50) blends via DSC, DMA and BDS

Literature on S-SBR/BR blends suggests that they are conditionally compatible. In particular, it has been reported for SBR/BR blends that a high-vinyl SBR is miscible with high-cis BR due to the repulsion between the vinyl and styrene units on the same SBR chain [27-29]. Therefore, a S-SBR with high-vinyl (50%) content and a BR with high-cis (>96%) and low-vinyl (<1%) content were chosen for this study. It was anticipated that a blend of these two polymers is miscible.

A combination of DSC, DMA, on the one hand and BDS on the other hand has been utilized to study the phase dynamics of the individual components in the S-SBR/BR blends. In addition to the blends, the pure elastomers (S-SBR and BR) were also analyzed. A single transition corresponding to the glass transition (α -relaxation) can be observed for both S-SBR and BR: Figure I. A peculiar crystallization peak was detected for BR due to its ability to crystallize. In the DSC and DMA curves, the peak corresponding to the crystallization of BR is noted at approximately $-40\text{ }^{\circ}\text{C}$. This is seen in the DSC curve as an exothermic peak at that temperature and in the DMA curve as a shoulder to the α -relaxation process on the left hand side: Figures I and II. In all blends, single DSC transitions as well as single $\tan \delta$ peaks from the dynamic mechanical studies are obtained. These results indicate miscibility in the blends. However, the single transitions from DSC and DMA measurements limit a deeper study into the phase preference of the TDAE oil in the oil-extended blends using these techniques.

Figure III shows a representative 3D curve as obtained from BDS for the S-SBR/BR (50/50) blend without TDAE. A 3D curve gives the opportunity to visualize the α -

relaxation process in terms of variation in ϵ'' on a frequency and temperature scale. A single broad and asymmetric relaxation can be noted in the temperature range covered, which can be associated with the α -relaxation. The maximum of the α -relaxation moves to higher temperatures with increasing frequency. This broad, asymmetric dielectric loss peak can be assigned to the combined contribution of both S-SBR and BR in the 50/50 blend. Although not shown here, the 3D curves for the oil-extended blends also exhibit only one broad relaxation. These single peaks are further analyzed and de-convoluted into the phase dynamics of the individual components of the blends, in such a way that the phase preference of the TDAE oil can be estimated.

3.2 Phase dynamics of S-SBR/BR (50/50) blends studied by BDS

This section discusses the fitting protocol which is devised to resolve the individual contribution of the S-SBR and BR phases to the α -relaxation of the blends. The dielectric loss vs. frequency spectra obtained from BDS were fitted using the Havriliak-Negami (HN) equation [30], which describes a dielectric relaxation process in terms of a characteristic relaxation time at the frequency of the maximum loss. The HN equation reads as follows,

$$\epsilon_{\text{HN}}^*(\omega) = \epsilon_{\infty} + \frac{\Delta \epsilon}{[1+(i\omega \tau_{\text{HN}})^b]^c} \quad (I)$$

where, τ_{HN} is the characteristic HN relaxation time, which represents the most probable relaxation time from the relaxation time distribution function, ω is the angular frequency, $\Delta \epsilon$ is the relaxation strength ($\Delta \epsilon = \epsilon_s - \epsilon_{\infty}$), where ϵ_{∞} and ϵ_s are the

unrelaxed and relaxed values of the dielectric constant respectively, $\epsilon_{HN}^*(\omega)$ is the frequency dependent Havriliak-Negami complex dielectric permittivity, and b and c are shape parameters, which describe the symmetric and asymmetric broadening of the relaxation time distribution function, respectively.

τ_{HN} is related to the relaxation time of maximum loss, τ_{max} and frequency of maximum loss [31], $F_{max} = 1/2\pi\tau_{max}$ by the following equation:

$$\tau_{max} = \frac{1}{2\pi F_{max}} = \tau_{HN} \left[\sin \frac{b\pi}{2+2c} \right]^{-\frac{1}{b}} \left[\sin \frac{bc\pi}{2+2c} \right]^{\frac{1}{b}} \quad (II)$$

Figure IV describes the dielectric loss plotted vs. the frequency for the pure polymers S-SBR and BR and for the S-SBR/BR (50/50) blends. These curves are normalized to the ϵ''_{max} for ease of comparison. The maximum of the dielectric loss moves to higher frequencies for all systems, pure polymers and blends, as the temperature increases. This shift in the frequency of the maximum loss gives evidence for these relaxation processes to be thermally activated [32].

The curve for pure S-SBR, Figure IV.A has a very symmetrical shape which is characteristic for a dielectric relaxation spectrum. For BR there is a shoulder on the left hand side due to the crystallization behavior of this elastomer, as already measured by DSC and DMA: Figures I and IV.B. A more detailed description of the DSC, DMA and BDS-based analysis of the pure polymers can be found in a previous publication [24].

With respect to the non-oil-extended blend it can be noted that the dielectric spectra are considerably broader and situated in between those of the two pure S-SBR and BR: Figure IV.C. Furthermore, the loss peak narrows as the temperature increases. These are well-known properties of dielectric spectra for miscible blends [33], thus emphasizing the miscibility of the S-SBR/BR (50/50) blends selected in this study. Similar behavior was also found in the TDAE-oil-extended blends: Figures IV.D and IV.E.

The dielectric response of a miscible blend expressed as a combined broad relaxation can be de-convoluted into its individual contributions using a HN-equation based fitting protocol [6,26]. Therefore, such a protocol was applied to the dielectric data of all the blends studied. During the HN-equation based fitting process, an appropriate fit of the measurement data for blend samples could not be obtained using a single HN-equation. This can most likely be attributed to the presence of two types of elastomers having different characteristic relaxation behaviors. Therefore, two HN-equations which can describe the relaxation behavior of the two elastomeric phases in the blends were used to fit the measurement data. The success of the fittings done using two HN-equations justifies the presence of two hidden relaxations arising from S-SBR and BR phases in the blends. These phases are referred to as α and α' , assigned to the BR and S-SBR phases, respectively, in decreasing order of frequency. At a fixed temperature, the BR phase is assigned to the relaxation appearing at higher frequency due to the greater mobility of the more linear BR chains compared to the more restricted S-SBR. While the steric hindrances in S-SBR chains due to the presence of the styrene-groups in the main chain cause a slowdown in its dynamics.

The fitted curves with the deconvoluted relaxation processes assigned to S-SBR (α') and BR (α), at a selected temperature $T = -30\text{ }^\circ\text{C}$ are shown in Figure V. This temperature was chosen because at this point the dielectric relaxation is clearly observable as a well-resolved peak in the frequency window. In all the curves, the collective relaxation spectrum is shown, which was fitted and deconvoluted into the two individual relaxation processes depicted as dashed lines. A conductivity contribution, shown as dotted line, was used to achieve a better fit of the low frequency tail of the dielectric spectra.

The relaxation parameters $\Delta\varepsilon_{(\alpha)}$, $\Delta\varepsilon_{(\alpha')}$, b , b' , c , c' , $\tau_{\text{HN}(\alpha)}$, and $\tau_{\text{HN}(\alpha')}$ for each contribution were calculated: Table IV. It is very difficult to obtain a fit of the experimental data while using two HN-equations due the large number of parameters that can vary simultaneously during fitting. To overcome this, changes in the b and c parameters for the α phase were allowed, and the c' was fixed to 1 while b' was allowed to change for the α' phase [34]. This approach also helped to maintain a more symmetrical shape of the contributions and a narrower distribution of relaxation times.

A difference in the characteristic HN-relaxation time τ_{HN} of the individual components in the blend is observed as the amount of oil is varied. Both rubber phases show longer relaxation times with increasing amount of oil, evidencing the restrictive dynamics induced by the TDAE oil.

As described earlier, the HN-relaxation times for both the α and α' phase, $\tau_{\text{HN}(\alpha)}$ and $\tau_{\text{HN}(\alpha')}$, can be converted to the respective τ_{max} using equation II. Figure VI shows τ_{max} plotted as a function of the inverse temperature. The temperature dependence of τ_{max} for both the S-SBR and BR phases follows the Vogel-Fülcher-Tamman (VFT) equation [35-37] expressed as:

$$\tau_{\text{max}} = \tau_0 \exp\left(\frac{B}{T-T_0}\right) \quad (\text{III})$$

Where τ_{max} is the relaxation time at the frequency of maximum loss, τ_0 and B are empirical parameters, and T_0 is the so-called ideal glass transition or Vogel temperature, which is generally 30-70 K below T_g [35]. To avoid the effect of misleading parameters, an empirical value of $\log \tau_0 = 14$ was adapted for the data fitting using the VFT equation, based on the approach proposed by Angell [38].

The effect of oil on the S-SBR (α') and BR (α) phases in the blend can be further interpreted based on Figure VI.B. The relaxation time curves of the two effective phases are placed apart from each other and seem to converge at higher temperatures, which is a characteristic feature of the segmental dynamics of polymeric chains as well as of VFT curves, due to the cooperative nature of the segmental relaxations [39]. This trend is observed independently of the amount of oil present in the blend. It can also be noted that the curves corresponding to the individual phases within the blends are situated between those of the pure polymers: compare Figure VI.A and VI.B, confirming the miscibility of the S-SBR/BR blend studied [6,26,33].

Another interesting observation can be obtained from comparison of Figure VI.A and Figure 6B and the effect of oil content. With regard to the pure polymers, Figure VI.A, the shift of the curves for oil-extended BR is towards lower inverse temperature: towards the oil, which indicates a restricting effect on the segmental dynamics of the BR chains as the amount of oil increases. For S-SBR there is no significant change in the dynamics with oil content, where the S-SBR in its pure and extended form has more restricted dynamics than the BR or the TDAE oil. Ideally, the two phases in the blend would be expected to behave as their pure components. It turns out that a clear restricting effect is observed in both effective phases as oil content increases: Figure VI.B. Moreover, the S-SBR phase in the blends has relaxation times very close to those of the TDAE, with more mobility than the corresponding pure polymer: Figure VI.A. S-SBR, pure and oil-extended, is situated on the left side of TDAE: more restricted, Figure VI.A, while the S-SBR phase in the blend is on the right side of TDAE: less restricted, Figure VI.B. Summarizing, two conclusions can be extracted from these results. First, the effect of TDAE oil is more pronounced on BR than on S-SBR; secondly, in S-SBR/BR oil-extended blends, the higher mobility of the BR phase affects the dynamics of the S-SBR phase to a larger extent than the oil itself, increasing its mobility compared to the pure polymer.

The effective T_g (T_g^{eff}) of the two phases in each blend were subsequently estimated as the temperature at $\tau_{\text{max}} = 100$ s, which is the convention for estimating the T_g by BDS [40], and compiled in Table V. A clear shift towards higher T_g^{eff} for the respective S-SBR and BR phases is observed as oil content increases, where the degree of shift is more pronounced for the BR phase compared to the S-SBR phase, as expected.

3.3 Theoretical approach to phase dynamics based on the Lodge and McLeish model

The T_g^{eff} of each elastomeric component in the blends obtained by BDS was compared to the T_g^{eff} calculated with theoretical models to describe the dielectric response of components in miscible blends [6,7,26]. The one used as part of the present study is the model for phase dynamics of miscible blends by Lodge and McLeish [26]. This model postulates that in a miscible blend, the local environment of a monomer of type A is, on average, richer in A compared to the bulk composition ϕ . A similar argument applies to another monomer of type B. It is a direct consequence of chain connectivity. By assigning a length scale or volume to a component dynamic mode, a 'self-concentration', ϕ_s can be estimated. In this model, the Kuhn length (l_K) is the chosen length scale:

$$\phi_s = \frac{C_\infty M_0}{k \rho N_{av} V} \quad (\text{IV})$$

where C_∞ is the characteristic ratio of the Kuhn length to the length of an average backbone bond, M_0 is the Kuhn element molar mass, k is the number of backbone bonds per repeat unit, V is the volume occupied by a Kuhn length's worth of monomers ($V \sim l_K^3$), ρ is the density and N_{av} is the Avogadro's number. The values assigned to these parameters for the two elastomers were taken from Fetters et al. [41]. Based on this, an effective local composition ϕ_{eff} was calculated from ϕ_s and ϕ :

$$\phi_{\text{eff}} = \phi_s + (1 - \phi_s)\phi \quad (\text{V})$$

The T_g^{eff} for each phase was then calculated using a modified Fox equation:

$$\frac{1}{T_g^{\text{eff}}(\phi_{\text{eff}}^{\text{(BR)}})} = \frac{\phi_{\text{eff}}^{\text{(BR)}}}{T_{g,\text{S-SBR}}} + \frac{1 - \phi_{\text{eff}}^{\text{(BR)}}}{T_{g,\text{BR}}} \quad (\text{VI})$$

where $T_g^{\text{eff(BR)}}$ is the effective T_g of the BR phase, $\phi_{\text{eff(BR)}}$ is the effective concentration of the BR phase, $T_{g,\text{S-SBR}}$ is the T_g of the S-SBR phase and $T_{g,\text{BR}}$ is the T_g of the BR phase. A similar equation is valid for the S-SBR phase for its $T_g^{\text{eff(S-SBR)}}$ calculation in the blend.

As suggested by the model, the T_g^{eff} of the component with lower T_g is closer to that of the pure polymer due to its flexible nature which leads to a larger ϕ associated with it. The higher T_g component is expected to have a lower ϕ associated with it, thus its dynamics and T_g^{eff} in the mixture would be more representative of the blend composition.

The T_g values calculated from this model for the studied blends and the experimentally obtained T_g for the individual phases are presented in Table V. The results obtained from BDS are in close correlation with the T_g^{eff} as calculated from the Lodge and McLeish model, with a small deviation for the BR phase. One possible reason for this deviation might be that the theoretical calculations are based on available data for typical BR polymers, whereas the polymers used in this study are new commercial grades. The agreement emphasizes the validity of the fitting protocol used and the deconvolution of the two phases in miscible S-SBR/BR (50/50) blends.

The calculated values of T_g^{eff} for the oil-extended compounds based on the theoretical model are not shown here since they were not quite coherent with the experimentally obtained data. This is primarily supposed to be due to the fact that the Lodge and McLeish model is applicable for the prediction of T_g^{eff} of two phases in a blend, not for the additional effect of process oils like TDAE.

4. CONCLUSIONS

S-SBR/BR (50/50) blends studied are miscible blends, as confirmed by the presence of a single glass transition signal observed by DSC, DMA and BDS. The segmental dynamics of the individual S-SBR and BR components in the S-SBR/BR (50/50) blend can be decoupled through the use of a fitting protocol based on the Havriliak-Negami equation, from the ‘apparently’ coupled relaxation dynamics, as observed from the BDS investigations. The effect of TDAE oil on the individual components in a S-SBR/BR (50/50) blend is clearly seen. However, no significant preference for a particular component was observed, except for a slightly larger effect on the BR contribution. The T_g^{eff} of the two components in the blend compounds studied were also calculated. Results suggest that the changes seen in T_g^{eff} for the individual components are a combined effect of: *i*) blending of two types of elastomeric chains and, *ii*) the addition of TDAE oil which may show a larger effect on a certain component within the blends. The values of T_g^{eff} calculated from BDS for the 50/50 blend without oil, correspond well with the Lodge and McLeish model for dynamics of miscible blends. The agreement of the T_g^{eff} of the individual blend components with the theoretical estimation confirms the

presence of miscibility in the blends. The work presented here establishes a platform for studying the effect of process oils on the individual phases of an elastomeric blend.

ACKNOWLEDGEMENTS

The authors are indebted to H&R Ölwerke Schindler GmbH (Hamburg, Germany) for their scientific, financial and materials support of the current project as well as the permission to publish this work. M. Hernández acknowledges the European Commission for a Marie Curie Fellowship (PIEF-GA-2013-623379).

REFERENCES

- [1] Fujimoto K.; Yoshimiya N. Blends of cis-1,4-Polybutadiene with Natural or Styrene Butadiene Rubber. *Rubber Chem. Tech.* **1968**, 41, 669-677.
- [2] Inoue T.; Shomura F.; Ougizawa T.; Miyasaka K. Covulcanization of Polymer Blends. *Rubber Chem. Tech.* **1985**, 58, 873-884.
- [3] Yoshimiya N.; Fujimoto J. Structure of Vulcanized and Unvulcanized SBR/BR Blends. *Rubber Chem Tech.* **1969**, 42, 1009-1013.
- [4] Furata I.; Hattori I.; Tsutsumi F. Experimental Study on the Miscibility and some physical Properties of the Blends of Natural Rubber and Polyisoprene with Various Contents of Vinyl-Isoprene. *ACS Rubber Division: Las Vegas, Nevada 1990*, Paper No. 49.

- [5] Ngai K.L.; Plazek D.J. In *Physical Properties of Polymers Handbook*, 2nd ed.; Mark J.E., Ed.; Springer: New York, U.S.A. 2007; p 456.
- [6] Shenogin S.; Kant R.; Colby R.H.; Kumar S.K. Dynamics of Miscible Polymer Blends: Predicting the Dielectric Response. *Macromolecules* **2007**, 40, 5767-5775.
- [7] Hirose Y.; Urakawa O.; Adachi K. Dielectric Study on the Heterogeneous Dynamics of Miscible Polyisoprene/Poly(vinyl ethylene) Blends: Estimation of the Relevant Length Scales for the Segmental Relaxation Dynamics. *Macromolecules* **2003**, 36, 3699-3708.
- [8] Madbouly S.A. Broadband Dielectric Spectroscopy for Poly(methyl methacrylate)/Poly(α -methyl styrene-co-acrylonitrile) Blend. *Polymer* **2002**, 34, 515-522.
- [9] Colmenero J.; Arbe A. Segmental Dynamics in Miscible Polymer Blends: Recent Results and Open Questions. *Soft Matter* **2007**, 3, 1474-1485.
- [10] Sengers W.G.F.; Wübbenhorst M.; Picken S.J.; Gotsis A.D. Distribution of oil in Olefinic Thermoplastic Elastomer Blends. *Polymer* **2005**, 46, 6391-6401.
- [11] Boese D.; Kremer F. Molecular Dynamics in Bulk cis-Polyisoprene as Studied by Dielectric Spectroscopy. *Macromolecules* **1990**, 23, 829-835.
- [12] Sauer B.B.; Avakian P.; Cohen G.M. Studies of Phase Separated Copolymer Blends using Thermally Stimulated Currents and Dielectric Spectroscopy. *Polymer* **1992**, 33, 2666-2671.
- [13] Cerveny S.; Bergman R.; Schwartz G.A.; Jacobsson P. Dielectric α - and β -Relaxations in Uncured Styrene Butadiene Rubber. *Macromolecules* **2002**, 35, 4337-4342.
- [14] Richter D.; Zorn R.; Farago B.; Frick B.; Fetters L.J. Decoupling of Time Scales of Motion in Polybutadiene Close to the Glass Transition. *Phys. Lett.* **1992**, 68, 71-74.

- [15] Richter D.; Monkenbusch M.; Arbe A.; Colmenero J.; Farago B. Dynamic structure factors due to relaxation processes in glass-forming polymers. *Physica B* **1998**, 1005, 241-243.
- [16] Litvinov V.M. EPDM/PP Thermoplastic Vulcanizates As Studied by Proton NMR Relaxation: Phase Composition, Molecular Mobility, Network Structure in the Rubbery Phase, and Network Heterogeneity. *Macromolecules* **2006**, 39, 8727-8741.
- [17] Saalwächter K.; Heuer A. Chain Dynamics in Elastomers As Investigated by Proton Multiple-Quantum NMR. *Macromolecules* **2006**, 39, 3291-3303.
- [18] He Y.; Lutz T.R.; Ediger M.D. Comparison of the Composition and Temperature Dependences of Segmental and Terminal Dynamics in Polybutadiene/Poly(vinylethylene) Blends. *Macromolecules* **2004**, 37, 9889-9898.
- [19] Luo H.; Klüppel M.; Schneider H. Study of Filled SBR Elastomers using NMR and Mechanical Measurements. *Macromolecules* **2004**, 37, 8000-8009.
- [20] Saalwächter K.; Klüppel M.; Luo H.; Schneider H. Chain Order in Filled SBR Elastomers: a Proton Multiple-Quantum NMR Study. *Appl. Magn. Reson.* **2004**, 27, 401-417.
- [21] Chung G.C.; Kornfield J. A.; Smith S.D. Component Dynamics in Miscible Polymer Blends: A Two-Dimensional Deuteron NMR Investigation. *Macromolecules* **1994**, 27, 964-973.
- [22] O'Brien J.; Cashell E.; Wardell G.E.; McBrierty V.J. An NMR Investigation of the Interaction between Carbon Black and cis-Polybutadiene. *Macromolecules* **1976**, 9, 653-660.
- [23] *Polymer Chemistry: The Basic Concepts*; Hiemenz P.C.; Marcel Dekker, Inc.: New York, U.S.A. 1984; p256.

- [24] Rathi A.; Hernández M.; Dierkes W.K.; Bergmann C.; Trimbach J.; Blume A. Structure-Property Relationships of Safe Aromatic Oil based Passenger Car Tire Tread Rubber Compounds. *Kautsch. Gummi Kunstst.* **2016**, 69, 22-27.
- [25] Schönhals A. In *Dielectric Spectroscopy of Polymeric Materials*; Runt J.P., Fitzgerald J.J., Eds.; American Chemical Society: Washington, DC, U.S.A. 1997; p 81.
- [26] Lodge T. P.; McLeish T. C. B. Self-Concentrations and Effective Glass Transition Temperatures in Polymer Blends. *Macromolecules* **2000**, 33, 5278-5284.
- [27] Marsh P.A.; Voet A.; Price L.D. Electron Microscopy of Heterogeneous Elastomer Blends. *Rubber Chem. Tech.* **1967**, 40, 359-370.
- [28] Marsh P.A.; Voet A.; Price L.D.; Mullens T.J. Fundamentals of Electron Microscopy of Heterogeneous Elastomer Blends. II. *Rubber Chem. Tech.* **1968**, 40, 344-355.
- [29] Sakurai S.; Izumitani T.; Hasegawa H.; Hasimoto T.; Han C.C. Small- Angle Neutron Scattering and Light Scattering Study on the Miscibility of Poly(styrene-ran-butadiene)/Polybutadiene Blends. *Macromolecules* **1991**, 24, 4844-4851.
- [30] Havriliak S.; Negami S. A Complex Plane Representation of Dielectric and Mechanical Relaxation Processes in some Polymers. *Polymer* **1967**, 8, 161-210.
- [31] Richter R.; Angell C.A. Dynamics of Glass-forming Liquids. V. On the link between Molecular Dynamics and Configurational Entropy. *J. Chem. Phys.* **1998**, 108, 9016-9026.
- [32] Teyssedre G.; Mezghani S.; Bernes A.; Lacabanne C. In *Dielectric Spectroscopy of Polymeric Materials*; Runt J.P., Fitzgerald J.J., Eds.; American Chemical Society: Washington, DC, U.S.A. 1997; p 227.
- [33] Schönhals A. In *Broadband Dielectric Spectroscopy*; F. Kremer, A. Schönhals, Eds.; Springer: Berlin Heidelberg GmbH, New York, U.S.A. 2003; p 272.

- [34] Hernández M.; Ezquerra T.A.; Verdejo R.; López-Manchado M.A. Role of Vulcanizing Additives on the Segmental Dynamics of Natural Rubber. *Macromolecules* **2012**, 45, 1070-1075.
- [35] Vogel H. The law of the Relation between the Viscosity of Liquids and the Temperature. *Phys. Z.* **1921**, 22, 645-646.
- [36] Fülcher G.S. Analysis of Recent Measurements of the Viscosity of Glasses. *J. Am. Cer. Soc.* **1925**, 8, 339-355.
- [37] Tammann G.; Hesse W. The dependence of viscosity upon the temperature of supercooled liquids. *Z. Anorg. Allg. Chem.* **1926**, 156, 245-257.
- [38] Angell C.A. Why $C=16-17$ in the WLF Equation is Physical and the Fragility of Polymers. *Polymer* **1997**, 38, 6261-6266.
- [39] Hernández M.; Valentin J.L.; López-Manchado M.A.; Ezquerra T.A. Influence of the vulcanization system on the dynamics and structure of natural rubber: Comparative study by means of broadband dielectric spectroscopy and solid-state NMR spectroscopy. *European Polymer Journal* **2015**, 68, 90-103.
- [40] Angell C.A. Relaxation in liquids, polymers and plastic crystals - strong/fragile patterns and problems. *J. Non-Crystalline Solids* **1991**, 131, 13-31.
- [41] Fetters L.J.; Lohse D.J.; Colby R.H. In *Physical Properties of Polymers Handbook*, 2nd ed.; Mark J.E., Ed.; Springer: New York, U.S.A. 2007; p 447.

Table I. Reported properties of BR, S-SBR and TDAE oil.

	S-SBR	BR	TDAE
Styrene (wt %)	21	-	-
1,2-vinyl (%)	50	<1	-
cis-1,4 (%)		>96	-
trans-1,4 (%)	29*	~2	-
Weight average molecular weight (M_w)(kg.mol⁻¹)	475	460	-
Number average molecular weight (M_n)(kg.mol⁻¹)	315	135	-
Glass transition temperature (T_g) (°C)	-25	-109	-49

*29% is the combined contribution of cis-1,4 and trans-1,4 in the S-SBR microstructure.

Table II. Mixing Formulation.

Component	(phr)
BR	50
S-SBR	50
Zinc Oxide	4
Stearic Acid	3
N-cyclohexyl-2-benzothiazole sulfenamide (CBS)	2.5
Sulfur	1.6
TDAE	0/10/20

Table III. Mixing Protocol.

1st Stage: Internal Mixer			2nd Stage: Two-
Brabender Plasticorder 350S			roll mill
Rotor speed: 50 RPM; Temperature: 50 °C; Fill factor: 0.7			Polymix 80T
			Friction ratio:
			1.25:1; ca. 40°C
0 phr TDAE	10 phr TDAE	20 phr TDAE	All samples
(Min. sec.)	(Min. sec.)	(Min. sec.)	(Min. sec.)
0.30 Add Polymers	0.30 Add Polymers	0.30 Add Polymers	0.30 Add Curatives
1.30 Add ZnO and	1.30 Add ZnO and	1.30 Add ZnO and	5.00 Dump
Stearic acid	Stearic acid	Stearic acid	
4.00 Dump	2.40 Add 3/4 th	2.40 Add 3/8 th	
	TDAE	TDAE	
	5.00 Add 1/4 th	5.00 Add 3/8 th	
	TDAE	TDAE	
	7.00 Dump	8.00 Add 1/4 th	
		TDAE	
		10.30 Dump	

TABLE IV. HN-fitting parameters for the deconvoluted relaxation spectra of S-SBR/BR (50/50) blends with varying concentrations of TDAE at T = -30 °C.

Compound	0 phr TDAE	10 phr TDAE	20 phr TDAE
$\Delta\epsilon_{\alpha}$	0.23	0.68	0.25
$\Delta\epsilon_{\alpha'}$	0.09	0.28	0.13
$\tau_{HN}(\alpha)$ (s)	1.38×10^{-4}	1.51×10^{-4}	2.00×10^{-4}
$\tau_{HN}(\alpha')$ (s)	5.32×10^{-4}	6.50×10^{-4}	1.10×10^{-3}
b	0.61	0.69	0.58
b'	0.43	0.46	0.44
c	0.13	0.11	0.23
c'	1	1	1

TABLE V. Comparison of the T_g^{eff} of the S-SBR and BR phases as calculated by the Lodge and McLeish Model and experimentally obtained from BDS.

Compound	Phase	T_g^{eff} (Model based)	T_g^{eff} (BDS)
0 phr TDAE	S-SBR	-42 °C	-43 °C
	BR	-60 °C	-69 °C
10 phr TDAE	S-SBR	-	-38 °C
	BR	-	-58 °C
20 phr TDAE	S-SBR	-	-36 °C
	BR	-	-54 °C

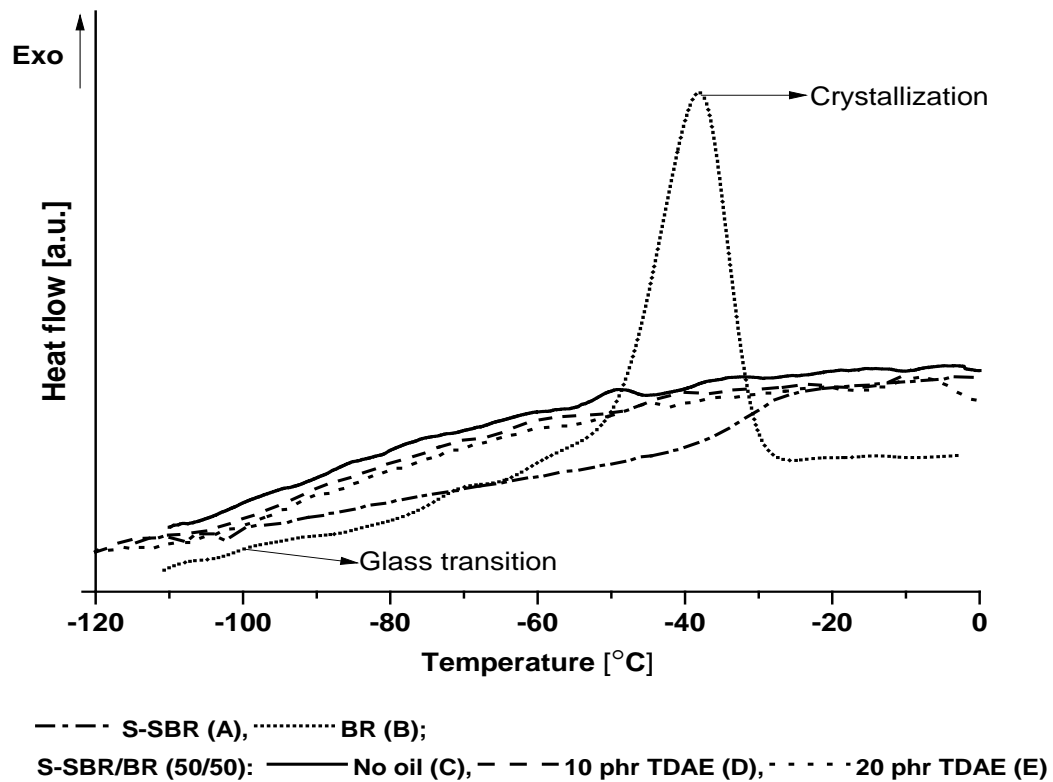


Figure I. DSC curve for pure polymers: A) S-SBR, B) BR; and for S-SBR/BR (50/50) blends with: C) 0 phr TDAE, D) 10 phr TDAE, and E) 20 phr TDAE.

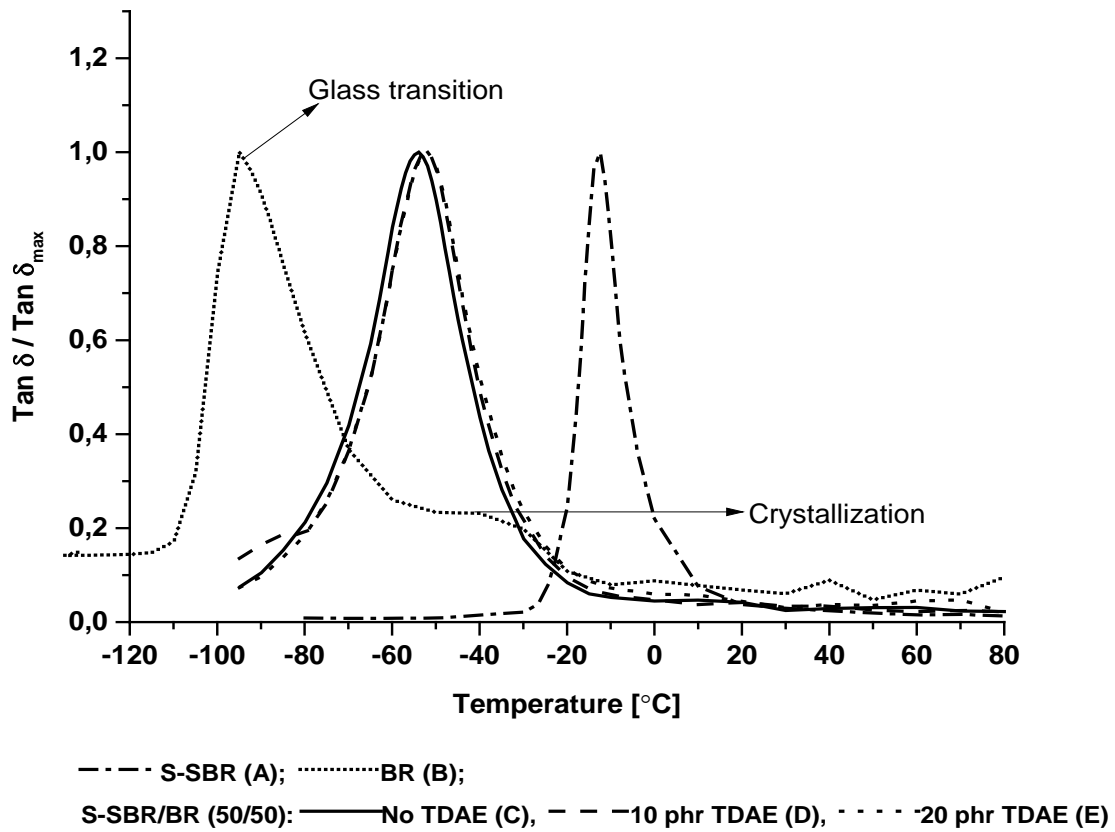


Figure II. $\tan \delta / \tan \delta_{\max}$ vs. Temperature curve for the pure polymers: A) S-SBR, B) BR; and for S-SBR/BR (50/50) blends with: C) 0 phr TDAE, D) 10 phr TDAE, and E) 20 phr TDAE.

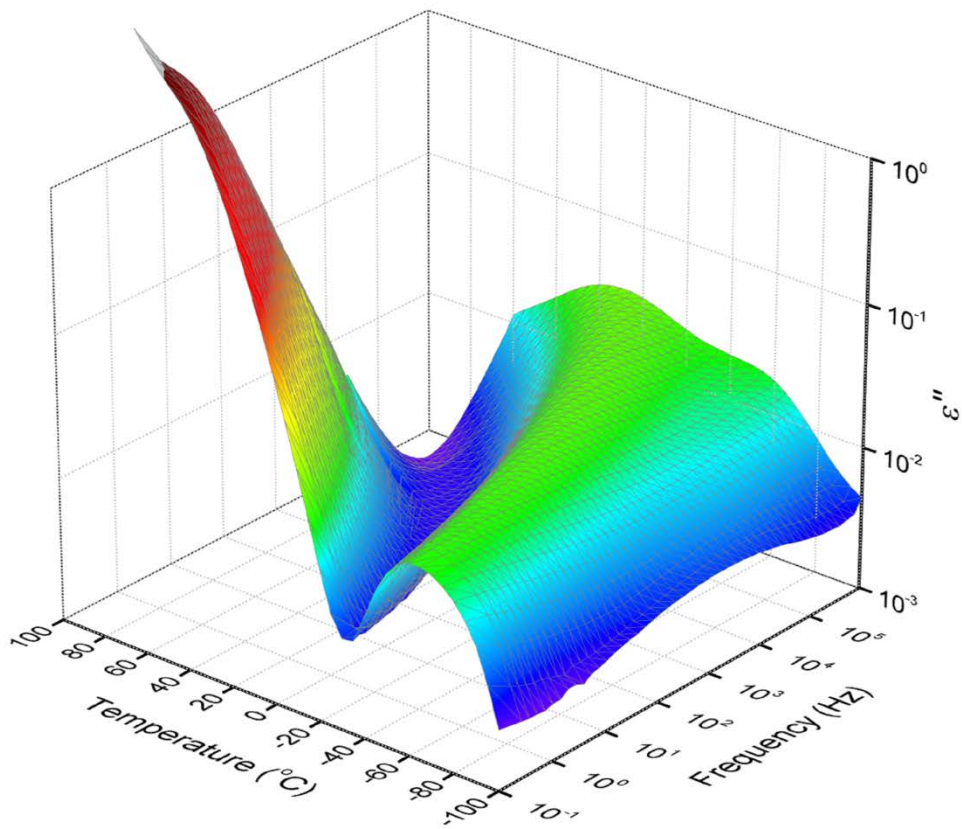


Figure III. 3D representation of the dielectric loss in the region of the α -relaxation of S-SBR/BR (50/50) blend as obtained from BDS.

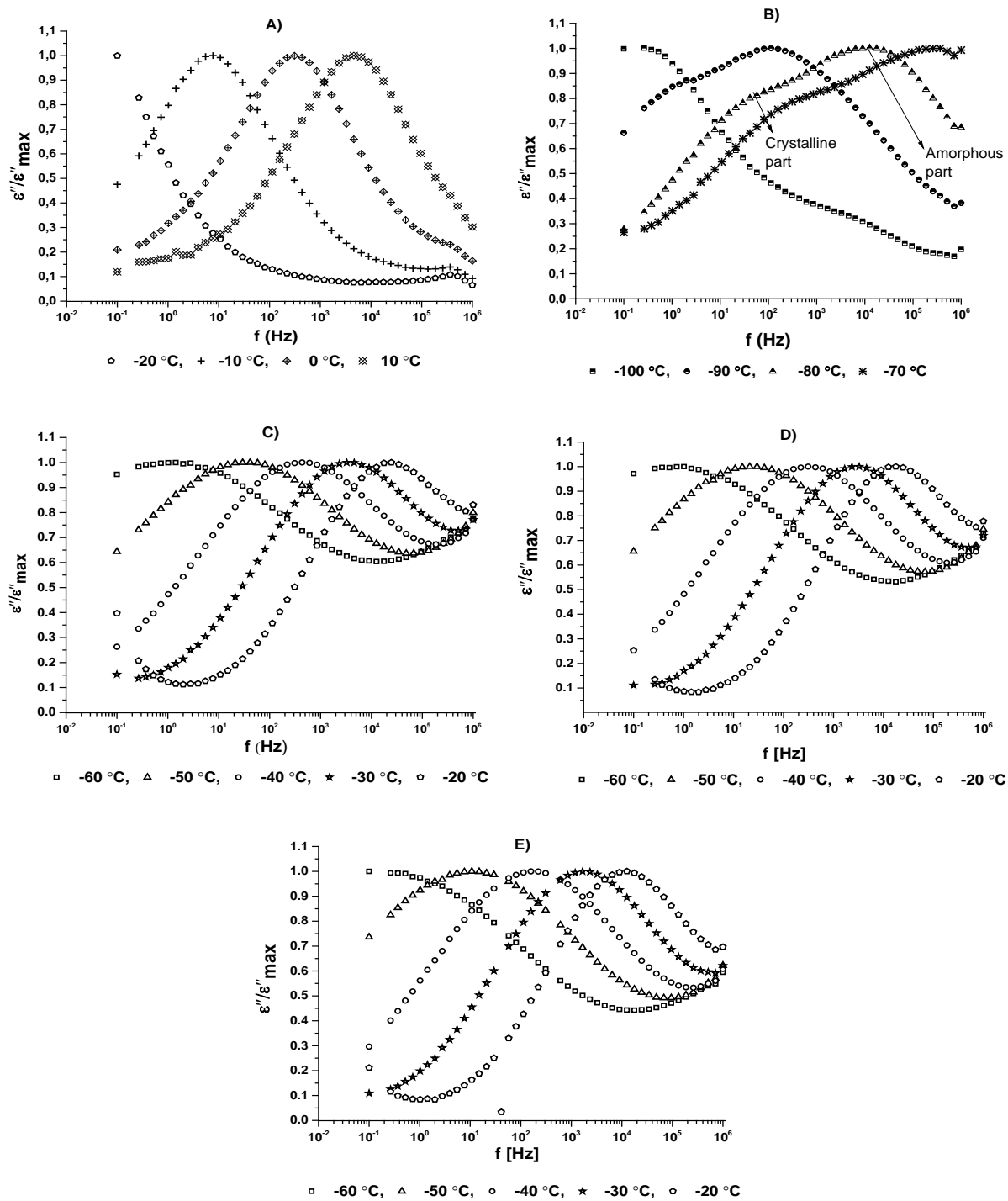


Figure IV. Normalized ϵ'' versus frequency in the region of the α -relaxation for pure polymers: A) S-SBR, B) BR; and for the S-SBR/BR (50/50) blends with: C) 0 phr TDAE, D) 10 phr TDAE, and E) 20 phr TDAE.

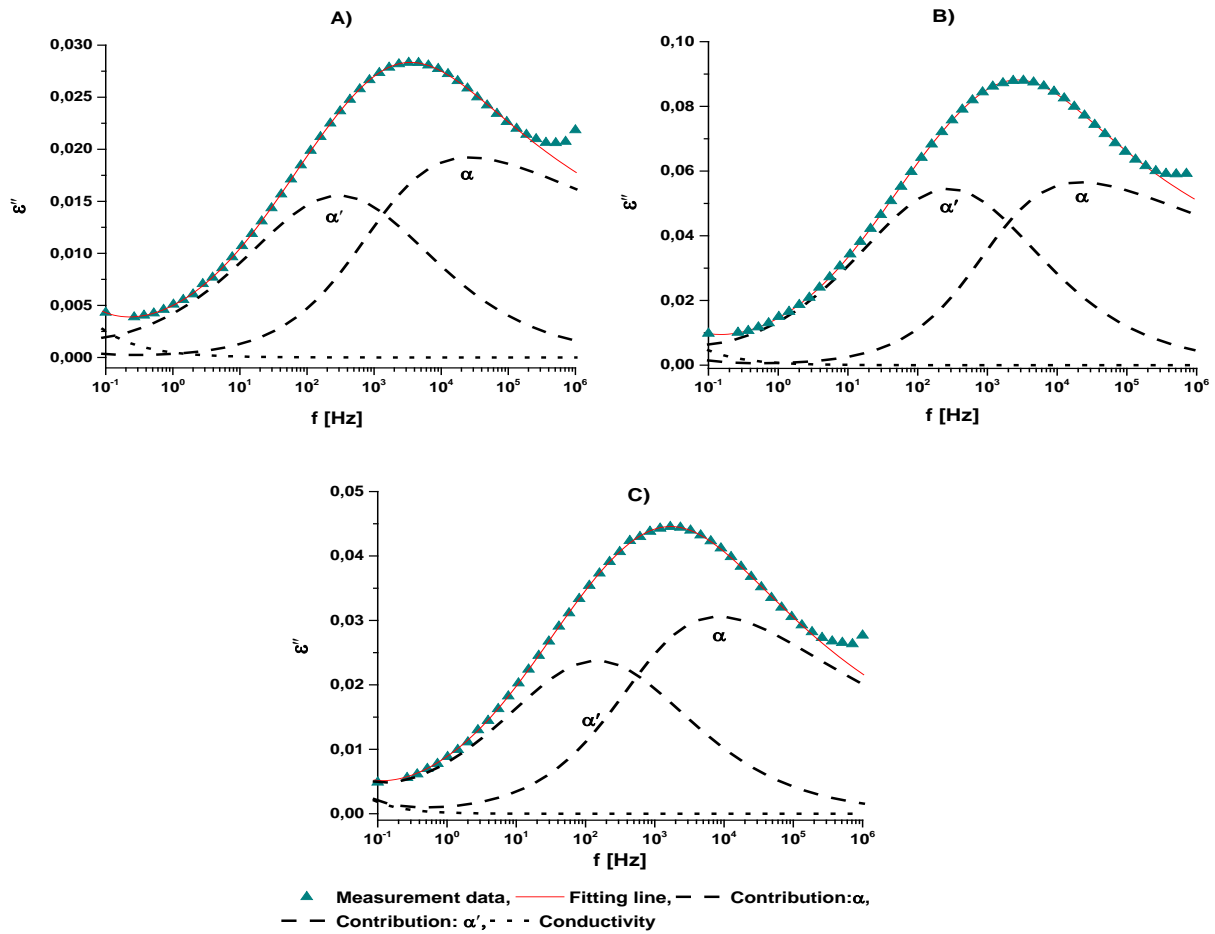


Figure V. Deconvolution results from fitting of the α' and α phases using 2 Havriliak-Negami (HN) equations for the S-SBR/BR (50/50) blends with: A) 0 phr TDAE, B) 10 phr TDAE, and C) 20 phr TDAE, at $T = -30\text{ }^{\circ}\text{C}$.

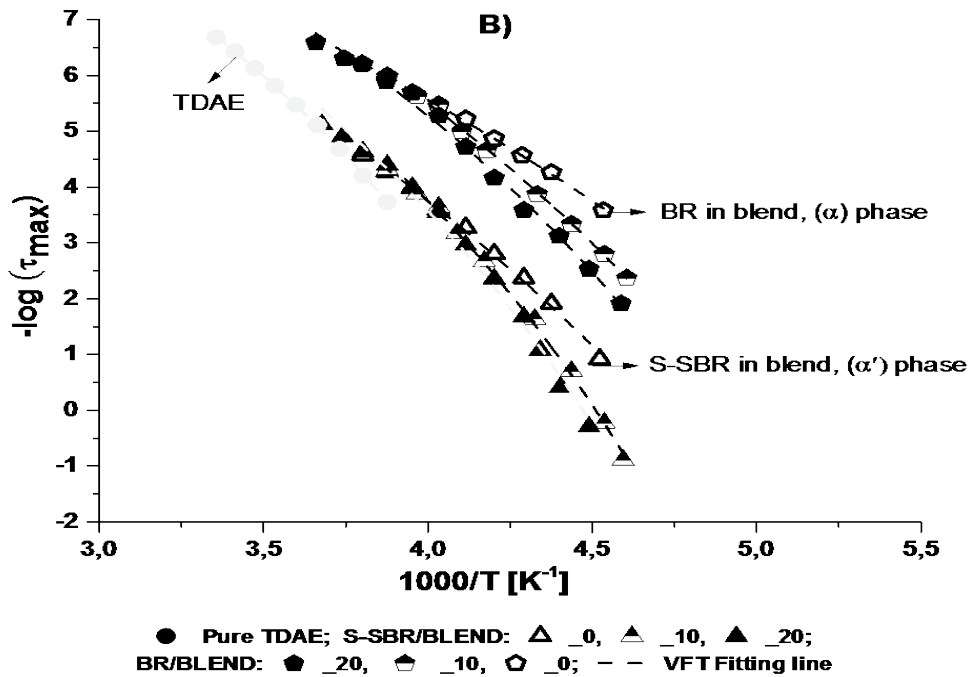
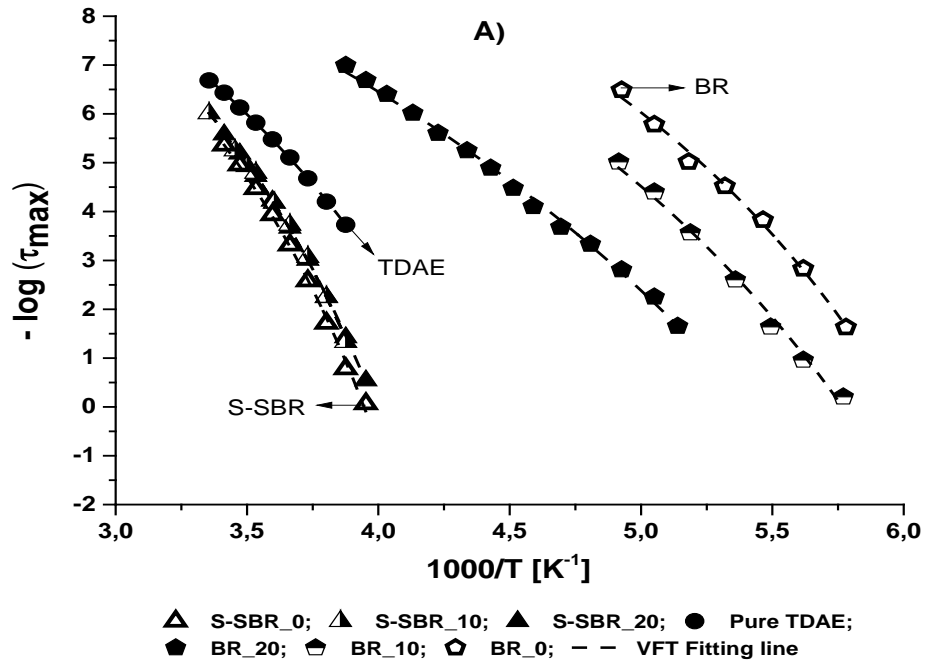


Figure VI. Temperature dependence of the average relaxation times of: A) Pure elastomers (S-SBR and BR) and B) S-SBR and BR phases in the S-SBR/BR (50/50) blends, with varied amounts of TDAE oil.